Contents lists available at CEPM

Computational Engineering and Physical Modeling

Journal homepage: www.jcepm.com

Cylindrical Bending of Power Law Varied Functionally Graded Laminate Subjected to Thermo-Mechanical Loading

S. P. Kulkarni[1*], S. S. Pendhari[2]

1. Research Scholar, Structural Engineering Department, Veermata Jijabai Technological Institute, Matunga, Mumbai 400 019, India
2. Associate Professor, Structural Engineering Department, Veermata Jijabai Technological Institute, Matunga, Mumbai 400 019, India

Corresponding author: *sspendhari@st.vjti.ac.in*

https://doi.org/10.22115/cepm.2020.243741.1124

ARTICLE INFO

Article history:
Received: 13 August 2020
Revised: 22 September 2020
Accepted: 06 October 2020

Keywords:
FGM;
Semi-analytical;
Thermo-mechanical loading;
2D domain;
Laminate.

ABSTRACT

In this paper, efforts have devoted to developing heat conduction formulation to determine the exact temperature for power law varied functionally graded (FG) laminate. Further, the semi-analytical approach has re-invented for displacement and stress analysis of FG laminate. This way of analysis involves solving of two-point boundary value problem (BVP) ruled by first-order ordinary differential equations (ODE's). Here material properties such as modulus of elasticity, coefficient of thermal expansion, and heat conductivity have considered being varied as per power law, whereas Poisson's ratio kept constant. The effect has undergone examination for applied transverse thermal loading and mechanical loading with the developed semi-analytical formulation. The observation of the effect of variation of volume fraction as per power law on through thickness temperature distribution along with consideration of exact temperature and with assumed power law temperature has carried out. Further corresponding thermal stress analysis and its comparison with numerical parametric studies lead to productive output in this area of research.

1. Introduction

Industries like aerospace, automotive, electronics, telecommunication, and defence always demand lightweight and tuff materials, and to fulfill these demands, a new class of composite

How to cite this article: Kulkarni SP, Pendhari SS. Cylindrical Bending of Power Law Varied Functionally Graded Laminate Subjected to Thermo-Mechanical Loading. Comput Eng Phys Model 2020;3(4):20–39. https://doi.org/10.22115/cepm.2020.243741.1124

material develops called functionally graded materials (FGM). These FGM's have generally made up of metals and ceramic, ranked smoothly in a particular direction(s). This unique material contains all the best properties of metals and ceramics like toughness, machinability, electrical conductivity, thermal resistance, corrosive resistance. Conventional composite materials drawbacks like debonding, interlaminar stresses, the formation of cracks, which usually occur due to the application of high static, thermal and mechanical loading, have eliminated. FGM also has applications in the area of biomedical, in the sports industry, in artificial body parts replacements. Generally, FGMs have in the form of beams, plates, and shells, and these have acted as thermal barriers between two extreme environmental conditions having substantial temperature differences. Some of the research related to the functionally graded (FG) laminates in which power-law varying material properties are subject to either mechanical, thermal, or both have discussed hereafter.

Chakraborty et al. [1] developed a new finite beam model which uses first-order shear deformation theory (FSDT). Here both exponential and power law varied material properties has used to identify the difference between pure metal and pure ceramic behaviour on FG material under static, free vibration and wave propagation problems. Benatta et al. [2] developed the flexural theory with higher-order shear deformation theory (HSDT) to avoid warping for short and symmetric FG beam under three-point bending. Kadoli et al. [3] studied the effect of power law exponent with a different combination of metal-ceramic on deflection and stress with the help of HSDT. Ben-Oumrane et al. [4] carried out the static analysis for S-FGM thick beam subjected to uniformly distributed loads. They have analysed the FG beam by using classical plate theory (CPT), FSDT, HSDT, and next unified kinematic formulation suggested and also compared. The exact solution for the behaviour of power law varied, exponential law varied, and sigmoid law varied FG beam and its properties on natural frequency under through thickness variation of temperature has given by Mahi et al. [5]. Kiani and Eslami [6] studied the buckling behaviour of the FG beam with the help of the Euler Bernoulli beam theory (EBT) under a different type of thermal loading. Wattanasakulpong et al. [7] used third-order shear deformation theory (TSDT) to study the buckling and vibration of power law varied FG beam. Guinta et al. [8] analysed the FG beam with refined axiomatic theories and studied free vibration characteristics. Here bending, axial, and natural torsional frequencies for slender and thick FG beam have derived. Ma and Lee [9] presented the governing differential equation for static and dynamic response of the FG beam with non-linear FOST beam theory and physical neutral surface for uniform in-plane thermal loading. Thai and Vo [10] have presented various HSDTs, partially similar to EBT, and studied bending and free vibration response of the FG beam. Further, Thai and Vo [11] presented nonlocal sinusoidal shear deformation theory for bending, buckling, and vibration of nanobeams. Ma and Lee [12] have developed the exact solution for the FG beam subjected to axial load with different boundary conditions. Simsek and Reddy [13] presented unified beam theory for static and free vibration analysis of FG microbeams based on modified couple stress theory. Li et al. [14] developed an analytical method for establishing a relationship between the bending of FGM Timoshenko beams and homogenous Euler – Bernoulli beams. Nazargah [15] has used a finite element approach for analysis of the FG beam subjected to bi-directional thermomechanical load. I-Ashmawy [16] has solved axially and transversally loaded thermo-mechanical FG beam with finite element (FE) models. This paper determines the dynamic response of axially and transversely loaded FG beam. Trinh et al. [17] carried out free vibration and buckling analyses of the FG beam subjected to thermo-

mechanical load. Here uniform, linear, and non-linear thermal loading have been considered with the help of the state-space method. Pietro et al. [18] used a unified approach to analyse the FG beam subjected to thermo-mechanical loading. This FG beam's materials have graded linear, parabolic, cubic, and thermal loading has derived through a heat conduction solution. Hui et al. [19] used a unified formulation for free vibration analysis of a three-dimensional sandwich beam with finite element modeling. Rajasekaran and Khaniki [20] developed a formulation for analysing a non-prismatic thin-walled beam, which has graded in two directions. This analysis has carried out for buckling and vibration behaviour of the FG Euler beam with finite element modeling.

Studying through past literature and understanding work done on FG materials so far, in this paper, efforts have made to evaluate the bending response of power law varying FG laminate for thermo-mechanical loading conditions. Here, it has attempted to extend the semi-analytical formulation developed by Pendhari et al. [21] for heat conduction and stress analysis of FG laminate. The necessary elasticity and heat conduction equations have used here for the development of semi-analytical methods includes defining two-point BVP governed by a group of coupled first-order ordinary differential equations (ODE's) (Equation 1) along with the thickness of a laminate on a basis from Kantorovich and Krylov [22] approach.

$$\frac{dy(z)}{dz} = D(z)\,y(z) + p(z) \tag{1}$$

Thermal loading has been determined as per the heat conduction equation and designed for accessing actual variation of temperature. Further, through the thickness, thermal change, as per simple power law, has also been discussed. Material properties here considered varied as per power law, and poisons ratio has held to be the same throughout the domain.

2. Mathematical formulations

Consider a single layer of thickness '*h*,' an FG laminate of length '*a*' in '*x*' direction with infinite extent along '*y*' direction. The support of FG laminate at two opposite edges (*x*=0, *a*) has shown. This laminate has subjected to mechanical and temperature load, which also varies only along with the length '*a*.' Under such a situation, laminate is the plane-strain condition of elasticity in the *x*-*z* plane (Figure. 1). The coefficient of thermal expansion (α), Elastic modulus (E), and coefficient of thermal conductivity (λ) have varied only through the thickness of laminate accordingly to a power law as,

$$\begin{bmatrix} E(z) \\ \alpha(z) \\ \lambda(z) \end{bmatrix} = \begin{bmatrix} E_b \\ \alpha_b \\ \lambda_b \end{bmatrix} + \left\{ \begin{bmatrix} E_t \\ \alpha_t \\ \lambda_t \end{bmatrix} - \begin{bmatrix} E_b \\ \alpha_b \\ \lambda_b \end{bmatrix} \right\} \left(\frac{z}{h} \right)^k \tag{2}$$

Where, E_b and E_t be Young's modulus of elasticity, α_b and α_t be constant of thermal expansion, λ_b and λ_t are the coefficient of thermal conductivity at the bottom and top surface of the laminate, respectively. Further, it has considered that the FG material has uniform

properties at every point, and the ratio of lateral strain versus linear strain is assumed to be constant throughout the thickness.

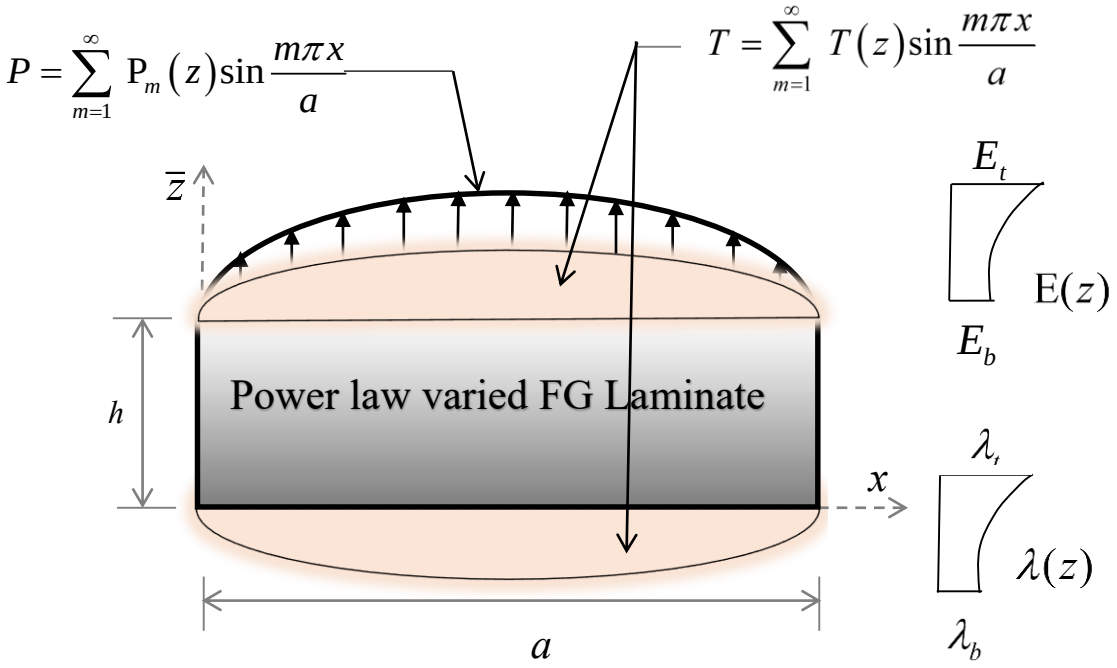

Fig. 1. FG laminate subjected to thermal and/or mechanical loading.

3. 2D Heat conduction Formulation by Semi-Analytical

The use of FG materials is primarily in situations where large temperature fields are experiencing on the structure, and hence, accurate determination of structural responses is of the utmost importance. This section is devoted to the discussion of the closed-form formulation for the 2D heat conduction equation. A thermal load and heat flux as defined in Eqn. (3) is assumed with only known temperature value at the top and bottom of the laminate surface $\left(T=T_b \text{ at } z=0 \text{ and } T=T_t \text{ at } z=h\right)$.

$$T(x,z)=\sum_{m=1}^{\infty} T(z)\sin\frac{m\pi x}{a} \quad \text{and} \quad q_z(x,z)=\sum_{m=1}^{\infty} q_z(z)\sin\frac{m\pi x}{a} \tag{3}$$

A governing two-dimensional (2D) steady-state heat conduction equation without internal heat generation is,

$$\lambda(z)\frac{\partial^2 T(x,z)}{\partial x^2}+\lambda(z)\frac{\partial^2 T(x,z)}{\partial z^2}=0 \tag{4}$$

As per Fourier's law of heat conduction, heat flux in direction x and z is given by,

$$q_x(x,z)=-\lambda(z)\frac{\partial T(x,z)}{\partial x} \qquad q_z(x,z)=-\lambda(z)\frac{\partial T(x,z)}{\partial z} \tag{5}$$

where, q_i = heat flux along x and z-axis ($i=x,z$) in Wm^{-2}

And, with the consideration, the heat flow maintains the amount of total heat in element zero, the equilibrium equation in 2D,

$$\frac{\partial q_z(x,z)}{\partial z}+\frac{\partial q_x(x,z)}{\partial x}=0 \tag{6}$$

Now, two variables viz. temperature field (T) and heat flux (q_z) are assumed as a primary variable. With the help of algebraic simplification of the Eqns. (5) and (6) a set of PDEs consisting of only two primary variables q_z and T are obtained.

$$\frac{\partial T(x,z)}{\partial z}=-\frac{1}{\lambda(z)}q_z(x,z) \qquad \frac{\partial q_z(x,z)}{\partial z}=-\lambda(z)\frac{\partial^2 T(x,z)}{\partial x^2} \tag{7}$$

Substituting Eqn. (3) and it's differential coefficients into Eqn. (7). The achievement of the following set of first-order ODE's as

$$\frac{dT_m(z)}{dz}=\frac{-1}{\lambda(z)}q_{zm}(z) \qquad \frac{dq_{zm}(z)}{dz}=-\lambda(z)\frac{m^2\pi^2}{a^2}T_m(z) \tag{8}$$

The governing two-point BVP in ODE's in the field $0\le z\le h$ with the known temperature at the upper and lower surface of FG laminate has given by Eqn. (8).

4. 2D Stress Analysis Formulation by Semi-Analytical formulation

As per the basic linear theory of elasticity, two-dimensional (2D) strain-displacement relationship, equilibrium equations, and constitutive relations in the thermo-elastic environment can be written as,

$$\varepsilon_x(x,z)=\frac{\partial u(x,z)}{\partial x} \qquad \varepsilon_z(x,z)=\frac{\partial w(x,z)}{\partial z} \qquad \gamma_{xz}(x,z)=\frac{\partial u(x,z)}{\partial z}+\frac{\partial w(x,z)}{\partial x} \tag{9}$$

$$\frac{\partial \sigma_x(x,z)}{\partial x}+\frac{\partial \tau_{xz}(x,z)}{\partial z}+B_x=0 \qquad \frac{\partial \tau_{zx}(x,z)}{\partial x}+\frac{\partial \sigma_z(x,z)}{\partial z}+B_z=0 \tag{10}$$

and,

$$\begin{Bmatrix}\sigma_x(x,z)\\ \sigma_z(x,z)\\ \tau_{xz}(x,z)\end{Bmatrix}^i=\begin{pmatrix}C_{11} & C_{12} & 0\\ C_{12} & C_{22} & 0\\ 0 & 0 & C_{33}\end{pmatrix}^i\begin{Bmatrix}\varepsilon_x(x,z)-\alpha(z)T\\ \varepsilon_z(x,z)-\alpha(z)T\\ \gamma_{xz}(x,z)\end{Bmatrix}^i \tag{11}$$

Here $\alpha(z)T$ are the free thermal strains that arise due to temperature variation. To avoid complications in the analysis, the body forces, B_x, B_z per unit volume in x and z directions, have neglected hereafter.

The above Eqns. (9), (10) and (11) contains eight unknowns in eight equations which have as u, w, ε_x, ε_z, γ_{xz}, σ_x, σ_z, τ_{xz}. After a simple algebraic reduction/manipulation of the basic elasticity equations, a set of PDEs involving only four dependent variables u, w, σ_z and τ_{xz} has received as follows.

$$\frac{\partial u(x,z)}{\partial z}=\frac{\tau_{zx}(x,z)}{C_{33}}-\frac{\partial w(x,z)}{\partial x}$$

$$\frac{\partial w(x,z)}{\partial z}=\frac{1}{C_{22}}\left[\sigma_z(x,z)-C_{21}\frac{\partial u(x,z)}{\partial x}+\alpha(z)T(x,z)(C_{21}+C_{22})\right] \quad (12)$$

$$\frac{\partial \tau_{zx}(x,z)}{\partial z}=\left[-C_{11}+\left(\frac{C_{12}C_{21}}{C_{22}}\right)\right]\frac{\partial^2 u(x,z)}{\partial x^2}-\frac{C_{12}}{C_{22}}\frac{\partial \sigma_z(x,z)}{\partial x}$$
$$-\left[\left(\frac{C_{12}C_{21}}{C_{22}}-C_{11}\right)\alpha(z)\right]\frac{\partial T(x,z)}{\partial x}$$

$$\frac{\partial \sigma_z(x,z)}{\partial z}=-\frac{\partial \tau_{xz}(x,z)}{\partial x}$$

And Equation (13) shows the second dependent variable, $\sigma_x(x,z)$ in the form of primary variables as,

$$\sigma_x(x,z)=C_{11}\frac{\partial u(x,z)}{\partial x}+C_{12}\frac{\partial w(x,z)}{\partial z}-(C_{11}+C_{12})\alpha(z)T(x,z) \quad (13)$$

With the help of boundary conditions at the support $x=0$ and a and Fourier trigonometric series expansion, the PDE's given in equation (12) can convert into coupled first-order ODE as,

$$u(x,z)=\sum_{m=1}^{\infty}u_m(z)\cos\left(\frac{m\pi x}{a}\right),\ w(x,z)=\sum_{m=1}^{\infty}w_m(z)\sin\left(\frac{m\pi x}{a}\right) \quad (14)$$

and from the fundamental relations of the theory of elasticity, it can be shown that,

$$\tau_{xz}(x,z)=\sum_{m=1}^{\infty}\tau_{xzm}(z)\cos\frac{m\pi x}{l} \qquad \sigma_z(x,z)=\sum_{m=1}^{\infty}\sigma_{zm}(z)\sin\frac{m\pi x}{l} \quad (15)$$

Further, applied transverse loading on the top of the FG laminate and temperature variation along the *x*-direction is also express in sinusoidal form as,

$$P(x,z)=\sum_{m=1}^{\infty}P_m(z)\sin\frac{m\pi x}{l} \quad \text{and} \quad T(x,z)=\sum_{m=1}^{\infty}T(z)\sin\frac{m\pi x}{l} \quad (16)$$

Putting Eqns. (14), (15) and (16) and its differential coefficients into Eqn. (12) Ordinary differential equations (ODEs), as mentioned in equation (17), have received.

$$\frac{du_m(z)}{dz}=\left(-\frac{m\pi}{a}\right)w_m(z)+\left(\frac{1}{C_{33}}\right)\tau_{xzm}(z)$$

$$\frac{dw_m(z)}{dz}=\left(\frac{C_{21}}{C_{22}}\frac{m\pi}{a}\right)u_m(z)+\left(\frac{1}{C_{22}}\right)\sigma_{zm}(z)+\left(\frac{C_{21}+C_{22}}{C_{22}}\right)\alpha(z)T(z)$$

$$\frac{d\tau_{xzm}(z)}{dz}=\left(\frac{C_{12}C_{21}}{C_{22}}-C_{11}\right)\left(\frac{m^2\pi^2}{a^2}\right)u_m(z)-\left(\frac{C_{12}}{C_{22}}\frac{m\pi}{a}\right)\sigma_{zm}(z) \quad (17)$$
$$-\left(\frac{C_{12}C_{21}}{C_{22}}-C_{11}\right)\left(\frac{m\pi}{a}\right)\alpha(z)T(z)$$

$$\frac{d\sigma_{zm}(z)}{dz}=\left(\frac{m\pi}{l}\right)\tau_{xzm}(z)$$

Eqn. (17) represents the governing two-point BVP in ODE's in the domain $0 \le z \le h$ with stress components known at the top and bottom surfaces of an FG laminate.

In the absence of a boundary layer effect, the numerical integration of the BVP has been defined in Eqns. (8), (17), and the associated boundary conditions can transform into a set of IVP's one non-homogeneous and $n/2$ homogeneous, equal to 2 and 4 for heat conduction and stress analysis formulation, respectively. This transformation of BVP to IVP for thermal and stress analysis have tabulated in Tables 1 and 2 successively. After this formation of a linear combination of one non-homogeneous and $n/2$ homogeneous solution, fulfilling boundary conditions $z = h$ have solved. These give rise to a system of $n/2$ linear algebraic equations, which determines the unknown $n/2$ components at the starting edge $z = 0$. Then a final numerical integration of Eqns. (8) (17) produces the required results. The fourth-order Runge-Kutta technique has been used here for numerical integration.

Table 1
Transformation of BVP into IVP's for thermal analysis

Integration No.	Bottom edge ($z = 0$)		Top edge ($z = h$)	
	$T(z)$	$q_z(z)$	$T(z)$	$q_z(z)$
1	Known	0 (Assumed)	M_{11}	M_{21}
2	0 (Assumed)	1 (Assumed)	M_{12}	M_{22}
3 (Final)	$T(0)$ (known)	$K1$	$T(h)$ (known)	$q_z(h)$

Table 2
Transformation of BVP into IVP's for stress analysis

Integration No.	Bottom edge $(z = 0)$				Top edge $(z = h)$				Load /Temp. Term
	u	w	τ_{xz}	σ_z	u	w	τ_{xz}	σ_z	
1	0 (Assumed)	0 (Assumed)	0 (known)	0 (known)	Y_{11}	Y_{21}	Y_{31}	Y_{21}	Include
2	1 (Assumed)	0 (Assumed)	0 (Assumed)	0 (Assumed)	Y_{12}	Y_{22}	Y_{32}	Y_{42}	Exclude
3	0 (Assumed)	1 (Assumed)	0 (Assumed)	0 (Assumed)	Y_{13}	Y_{23}	Y_{33}	Y_{34}	Exclude
4 (Final)	X_1	X_2	0 (known)	0 (known)	$u(h)$	$w(h)$	0 (known)	0 (known)	Include

5. Numerical studies

A computer code has developed based on the current formulation, further, with the help of this determination of accurate temperature distribution and thermal stress analysis of the FG laminate noted. For numerical study, the upper and lower surface of the laminate has been assumed to subject 20^0C and 300^0C temperature, respectively. Table 3 represents three material sets that have considered for study the effect of material properties on temperature distribution along with the thickness of a laminate. The top surface has a fully ceramic layer, and the bottom surface has a fully metallic layer, in between segments has graded with the

help of power indices (k). Numerical integration uses 20 to 30 steps through the thickness of the FG laminate.

Comparison between actual temperature distribution and assumed power law varied temperature distribution through the thickness of FG laminate have made all material sets and depicted in Figures 2 to 4. Further, to determine the thickness effect on this study, various aspect ratios (s) from 5 to 50 have investigated. From the graphs, it has been seen that the actual temperature profile for different aspect ratios (a/h) is almost the same, proves the independency of aspect ratios (a/h) on temperature distribution along with the FG laminate thickness for all material sets. However, noticeable differences have been observed for all material sets when through thickness temperature distribution obtained by heat conduction solution compared with simple assumed power-law varied temperature profile along with the FG laminate thickness. Further, the difference between actual and assumed temperature variations goes on reducing for material set A to C has observed, which showed the material dependency on temperature distribution. Next, it has also noted that the power index, (k) equal to 0, which represents ceramic, heat conduction solution gives linearly varied temperature distribution. Whereas, variation as per assumed power law gradation initially shows sudden jumps in results just up from the bottom surface of laminate along thickness direction and has remained constant further. As the value of power indexes (k) increases, temperature variation obtained through heat conduction solution showed convex nature up to power index (k) equal to 2.0, whereas temperature variation followed by the assumed power law equation shows the concave view up to power index (k) equal to 0.8. Further, for power law (k) index similar to or more than 10 representing metallic nature, a linear variation of temperature produced from heat conduction solution whereas the thickness variation of temperature as per assumed power law equation showed convexly.

Table 3
Material Properties

Set	Material Properties
a	At bottom, $z = 0 \Rightarrow$ Aluminium: $E = 70\ GPa$ $\mu = 0.3$ λ=204 K^{-1} $\alpha = 23 \times 10^{-6}\ W_m^{-1}K^{-1}$ At top, $z = h \Rightarrow$ Zirconia : $E = 151\ GPa$ $\mu = 0.3$ λ=2.09 K^{-1} $\alpha = 10 \times 10^{-6}\ W_m^{-1}K^{-1}$
b	At bottom, $z = 0 \Rightarrow$ Aluminium: $E = 70\ GPa$ $\mu = 0.3$ λ=204K^{-1} $\alpha = 23 \times 10^{-6}\ W_m^{-1}K^{-1}$ At top, $z = h \Rightarrow$ Alumina : $E = 380\ GPa$ $\mu = 0.3$ $\lambda = 10.40K^{-1}$ $\alpha = 7.4 \times 10^{-6}\ W_m^{-1}K^{-1}$
c	At bottom, $z = 0 \Rightarrow$ Monel : $E = 227.24\ GPa$ $\mu = 0.3$ λ=25 K^{-1} $\alpha = 15 \times 10^{-6}\ W_m^{-1}K^{-1}$ At top, $z = h \Rightarrow$ Zirconia : $E = 151\ GPa$ $\mu = 0.3$ λ=2.09 K^{-1} $\alpha = 10 \times 10^{-6}\ W_m^{-1}K^{-1}$

Ref. Kadoli et al. [3]

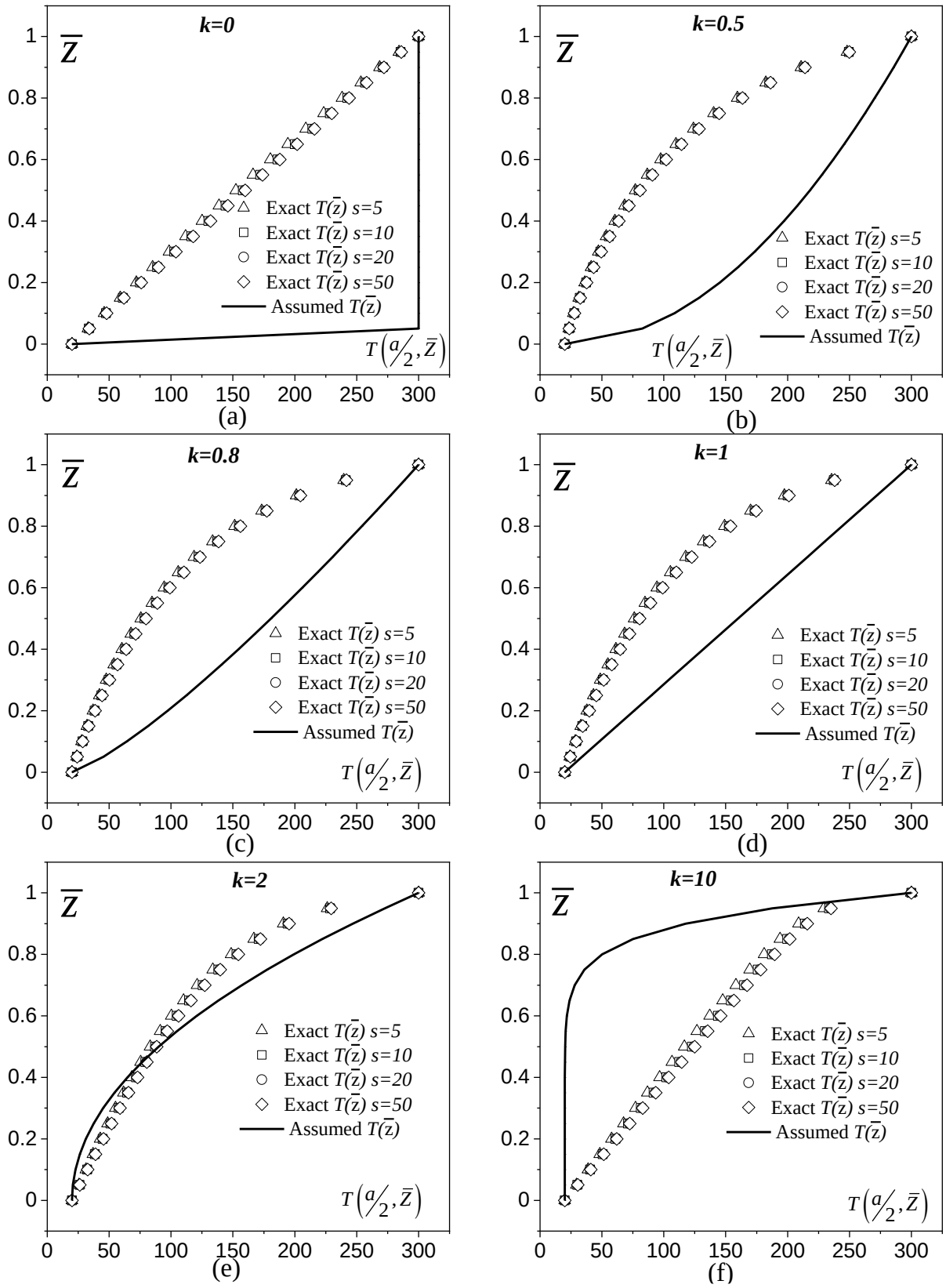

Fig. 2. Comparison between through thickness exact temperature variation and power law variation for various power index (*k)* of FG laminate Material set A].

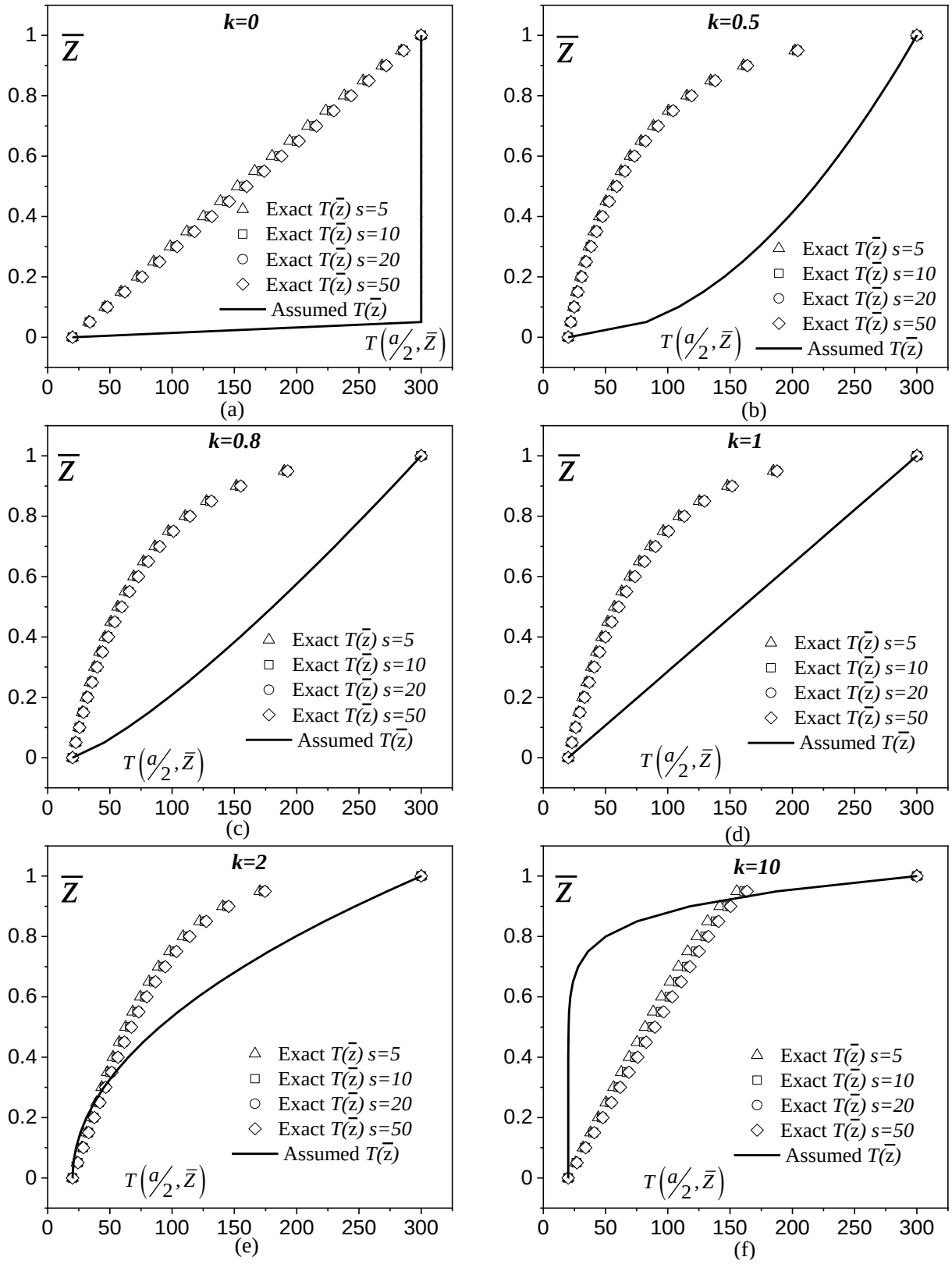

Fig. 3. Comparison between through thickness exact temperature variation and power law variation for various power index (*k*) of FG laminate [Material set B].

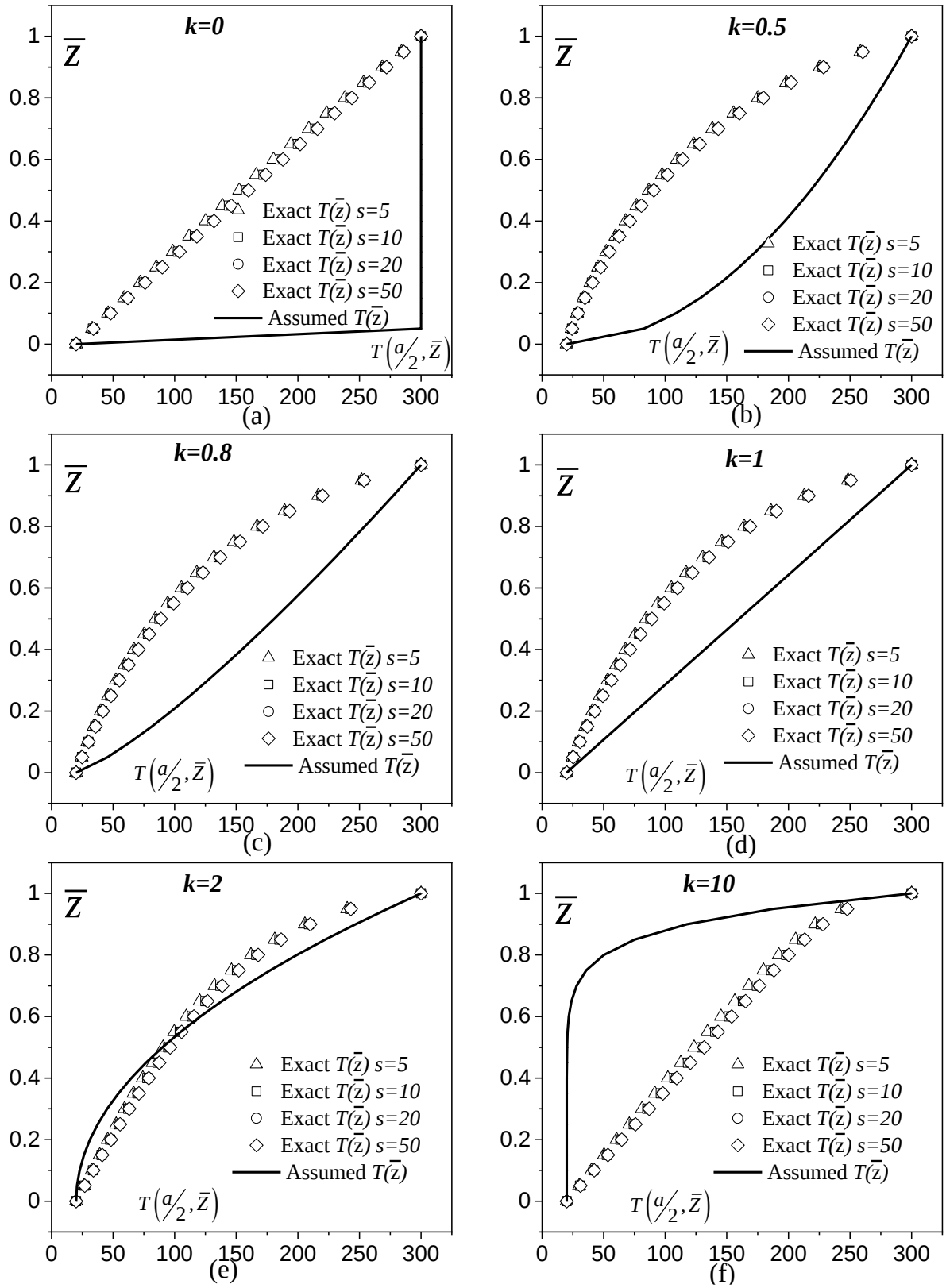

Fig. 4. Comparison between through thickness exact temperature variation and power law variation for various power index (*k)* of FG laminate [Material set C].

Thermal stress analyses for accurate through thickness temperature profile have obtained from heat conduction solution (Model 1) and assumed power law temperature profile (Model 2). All material sets and various aspect ratios (*a/h*) has analysed. Comparison and uniform presentation of numerical results has carried with the following normalization coefficients.

$$\bar{u} = \frac{100u}{\alpha_b T_b s^3} \quad ; \quad \bar{w} = \frac{10w}{\alpha_b T_b s^4} \quad ; \quad \bar{\sigma}_x = \frac{\sigma_x}{E_b \alpha_b T_b} \quad ; \quad \bar{\tau}_{xz} = \frac{s^2 \tau_{xz}}{E_b \alpha_b T_b} \tag{18}$$

After analysis, the results which received have tabulated in Table 4 and through thickness comparison between Model 1 and Model 2 for in-plane and transverse displacements $(\bar{u}_n, \bar{w}_n)$ and in-plane normal and transverse shear stresses $(\bar{\sigma}_x, \bar{\tau}_{xz})$ have depicted in Figure 5 to Figure 8 for material set C only. Figures 5 and 6 indicate through thickness variation of in-plane displacement followed a simple linear profile. In contrast, transverse displacement showed little curvature. The difference between Model 1 and Model 2, displacement values are very minimum for aspect ratio (s) 10, simulating moderately thick laminate. Further, the exact opposite pattern of variations had observed for in-plane normal stresses (Figure 7). The effect of aspect ratios (*s*) has absent for through thickness variation of in-plane normal stress $(\bar{\sigma}_x)$ obtained from Model 1 for all power law indices. Through thickness variations derived from Model 2 showed the dependency of aspect ratios only for ceramic reclining laminate (power index less than 1.0). Moreover, transverse shear stress $(\bar{\tau}_{xz})$ followed sinusoidal variations for both Model 1 and Model 2; however, in the opposite direction (Figure 8).

Further, the transverse mechanical load $P_0 = 1N/mm^2$ has applied on the top surface of FG laminate along with thermal effect, and stress analysis has performed for all material sets and transverse aspect ratio (*s*) 5, 10, 20, and 50. The following normalized coefficients have been used here for the comparison of the results.

$$s = \frac{a}{h} \qquad \bar{u} = \frac{u}{h\alpha_b T_b s^3} \qquad \bar{w} = \frac{w}{h\alpha_b T_b s^4} \qquad \bar{\sigma}_x = \frac{\sigma_x}{350 P_0 \alpha_b T_b s^2} \qquad \bar{\tau}_{xz} = \frac{\tau_{xz}}{140 P_0 \alpha_b T_b s} \tag{19}$$

In which bar over the variables defines its normalized value.

Response for in-plane displacement $(\bar{u})$, transverse displacement $(\bar{w})$, in-plane normal stress, $(\bar{\sigma}_x)$ and transverse shear stress $(\bar{\tau}_{xz})$ obtained from Exact and Assumed have documented in Tables 5. However, when the laminate is subject to thermal loading and mechanical loading, no significant differences have been seen for all parameters in the responses obtained from Exact and Assumed. These may be due to the neutralizing the overall effect of thermal loading by mechanical loading. However, investigation of the intensity of mechanical loading effects has neglected in the present studies.

Table 4.

Normalized in-plane and transverse displacements $(\bar{u}, \bar{w})$ and stresses $(\bar{\sigma}_x, \bar{\tau}_{xz})$ of FG laminate under thermal loading for material set A, B, and C.

s	k	Source	$\bar{u}_n\ (0, h\ \&\ 0)$		$\bar{w}_n\left(a/2, \max\right)$	$\bar{\tau}_{xz}\left(0, \max\right)$	$\bar{\sigma}_x\left(a/2, h\ \&\ 0\right)$	
Material set A								
5	0	Model 1	-8.304	-0.554	0.282	0.000	0.001	0.000
		Model 2	-8.573	-8.573	0.052	0.752	0.502	0.502
	0.5	Model 1	-5.187	-0.241	0.179	2.330	-5.804	-0.891
		Model 2	-9.537	-6.254	0.156	3.750	2.297	4.299
	0.8	Model 1	-5.216	-0.553	0.171	1.741	-5.748	-0.622
		Model 2	-9.862	-4.445	0.221	4.167	2.901	2.737
	1.0	Model 1	-5.289	-0.725	0.168	1.437	-5.613	-0.473
		Model 2	-9.951	-3.451	0.254	4.003	3.067	1.879
	2.0	Model 1	-5.811	-1.295	0.170	0.580	-4.641	0.019
		Model 2	-9.611	-0.649	0.326	1.774	2.434	-0.538
	10	Model 1	-8.519	-1.739	0.255	1.669	0.400	0.402
		Model 2	-5.785	0.511	0.221	3.617	-4.689	-1.540
Material set B								
5	0	Model 1	-6.119	-0.408	0.208	0.000	0.003	0.000
		Model 2	-6.317	-6.317	0.038	1.420	0.947	0.947
	0.5	Model 1	-5.174	-0.609	0.168	2.405	-4.502	-0.583
		Model 2	-7.143	-6.492	0.062	7.518	4.886	4.585
	0.8	Model 1	-5.320	-1.018	0.161	1.215	-3.809	-0.224
		Model 2	-7.583	-5.168	0.117	9.153	6.986	3.422
	1.0	Model 1	-5.454	-1.268	0.158	0.729	-3.167	-0.005
		Model 2	-7.771	-4.327	0.149	9.251	7.884	2.683
	2.0	Model 1	-6.253	-2.202	0.158	2.653	0.641	0.816
		Model 2	-7.981	-1.451	0.243	6.592	8.883	0.156
	10	Model 1	-10.46	-3.067	0.288	8.596	20.709	1.576
		Model 2	-5.855	0.599	0.225	3.930	-1.255	-1.645
Material set C								
5	0	Model 1	-4.824	0.746	0.196	1.802	-3.780	-0.762
		Model 2	-13.146	-13.146	0.080	0.296	0.198	0.198
	0.5	Model 1	-10.173	-0.191	0.360	1.272	-1.223	-0.934
		Model 2	-14.530	-5.794	0.349	1.720	0.859	3.902
	0.8	Model 1	-9.985	-0.432	0.346	1.177	-1.313	-0.726
		Model 2	-14.417	-3.441	0.415	1.499	0.805	1.871
	1.0	Model 1	-9.984	-0.568	0.342	1.076	-1.314	-0.609
		Model 2	-14.174	-2.346	0.439	1.170	0.689	0.926
	2.0	Model 1	-10.492	-1.037	0.346	0.506	-1.071	-0.204
		Model 2	-12.326	0.195	0.449	1.471	-0.194	-1.268
	10	Model 1	-14.376	-1.610	0.468	1.091	0.786	0.290
		Model 2	-5.444	0.311	0.207	3.152	-3.483	-1.368

Table 5

Normalized in-plane and transverse displacements $\left(\bar{u},\bar{w}\right)$ and stresses $\left(\bar{\sigma}_x,\bar{\tau}_{xz}\right)$ of FG laminate under thermomechanical loading for material set A, B, and C

s	k	Source	$\bar{u}_n\ \left(0,h\,\&\,0\right)$		$\bar{w}_n\left(a/2,\max\right)$	$\bar{\tau}_{xz}\left(0,\max\right)$	$\bar{\sigma}_x\left(a/2,h\,\&\,0\right)$	
Material set A								
5	0	Model 1	-2.583	2.561	1.799	0.031	3.830	-3.822
		Model 2	-2.586	2.481	1.775	0.031	3.834	-3.818
	0.5	Model 1	-2.989	3.558	2.281	0.031	4.434	-2.466
		Model 2	-3.032	3.498	2.277	0.031	4.499	-2.424
	0.8	Model 1	-3.144	3.920	2.464	0.031	4.665	-2.715
		Model 2	-3.190	3.881	2.467	0.031	4.734	-2.688
	1.0	Model 1	-3.221	4.095	2.555	0.031	4.780	-2.836
		Model 2	-3.268	4.067	2.561	0.031	4.850	-2.817
	2.0	Model 1	-3.457	4.533	2.809	0.031	5.132	-3.139
		Model 2	-3.495	4.539	2.823	0.031	5.189	-3.143
	10	Model 1	-4.221	4.959	3.256	0.030	6.270	-3.432
		Model 2	-4.194	4.981	3.254	0.030	6.230	-3.448
Material set B								
5	0	Model 1	-1.029	0.993	0.710	0.031	3.814	-3.806
		Model 2	-1.031	0.934	0.692	0.031	3.821	-3.798
	0.5	Model 1	-1.336	1.757	1.076	0.032	4.985	-1.244
		Model 2	-1.356	1.698	1.064	0.032	5.060	-1.202
	0.8	Model 1	-1.489	2.175	1.273	0.033	5.568	-1.538
		Model 2	-1.512	2.133	1.268	0.033	5.654	-1.508
	1.0	Model 1	-1.575	2.424	1.391	0.033	5.897	-1.712
		Model 2	-1.599	2.393	1.389	0.033	5.986	-1.691
	2.0	Model 1	-1.855	3.262	1.800	0.032	6.963	-2.302
		Model 2	-1.872	3.270	1.808	0.032	7.029	-2.307
	10	Model 1	-2.621	4.154	2.468	0.029	9.886	-2.929
		Model 2	-2.563	4.167	2.453	0.029	9.665	-2.938
Material set C								
5	0	Model 1	-4.728	4.714	3.303	0.031	9.046	-9.027
		Model 2	-4.732	4.591	3.267	0.031	9.054	-9.019
	0.5	Model 1	-3.997	3.400	2.592	0.031	7.650	-11.783
		Model 2	-3.991	3.353	2.589	0.031	7.733	-11.590
	0.8	Model 1	-3.839	3.204	2.463	0.031	7.348	-11.105
		Model 2	-3.884	3.174	2.467	0.031	7.433	-11.001
	1.0	Model 1	-3.764	3.128	2.407	0.031	7.204	-10.844
		Model 2	-3.806	3.111	2.414	0.031	7.284	-10.783
	2.0	Model 1	-3.532	2.964	2.259	0.031	6.760	-10.275
		Model 2	-3.550	2.976	2.268	0.031	6.795	-10.318
	10	Model 1	-3.042	2.752	2.013	0.031	5.822	-9.546
		Model 2	-2.952	2.772	1.990	0.031	5.652	-9.613

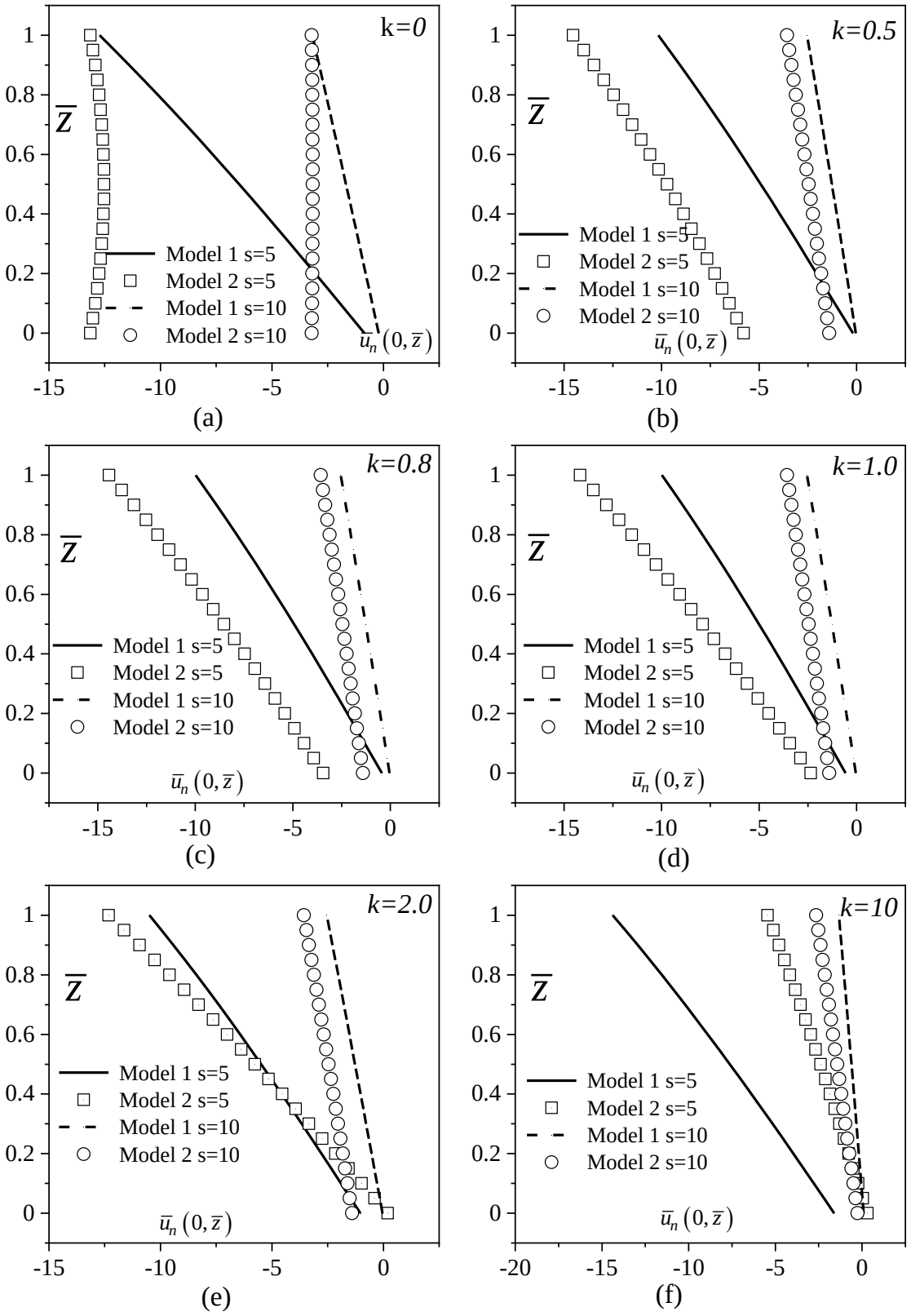

Fig. 5. Thickness variation of normalized in-plane displacement ($\overline{u}_n$) for various graded FG laminate [Material set C].

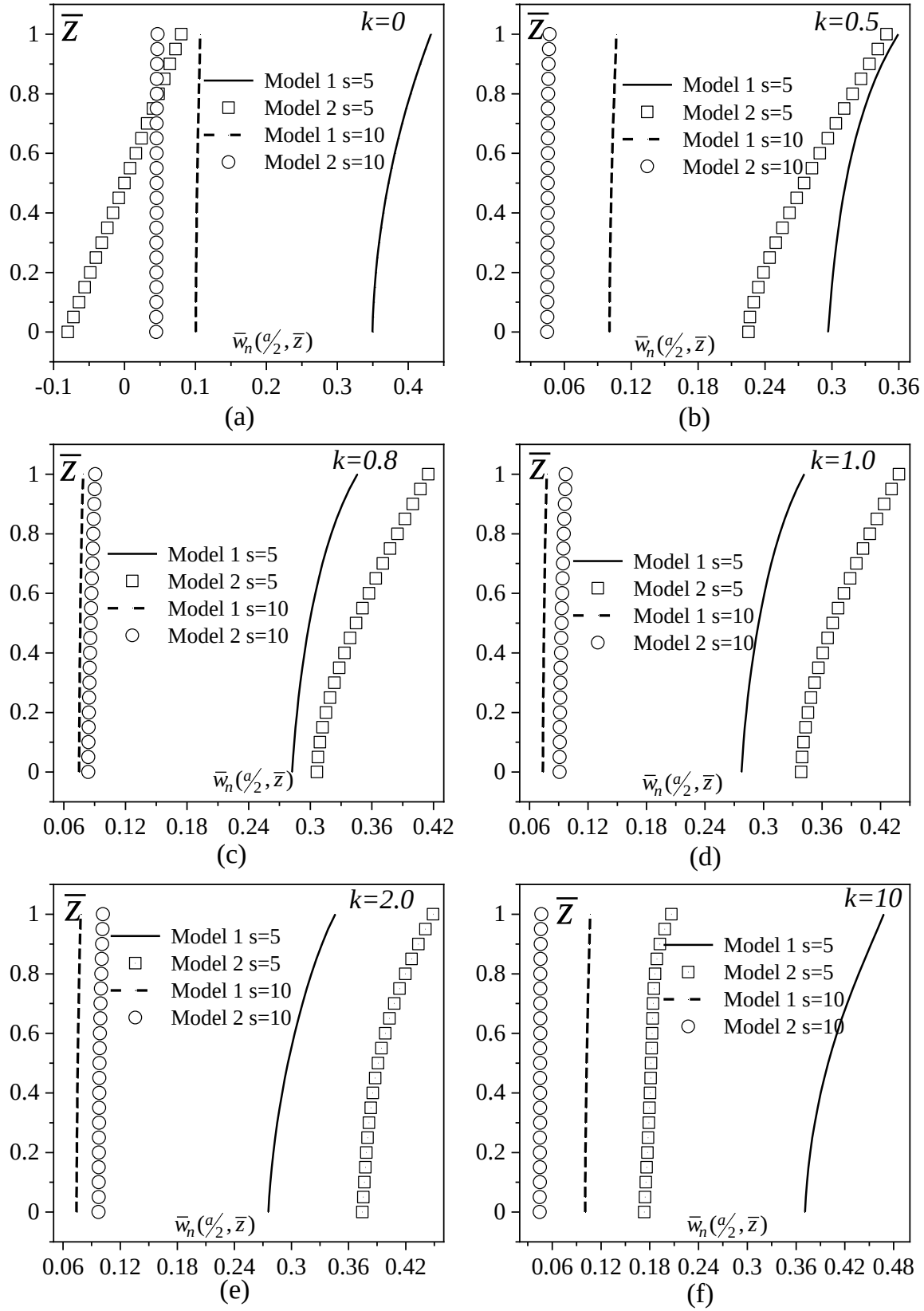

Fig. 6. Thickness variation of normalized transverse displacement ($\bar{w}_n$) for various graded FG laminate [Material set C].

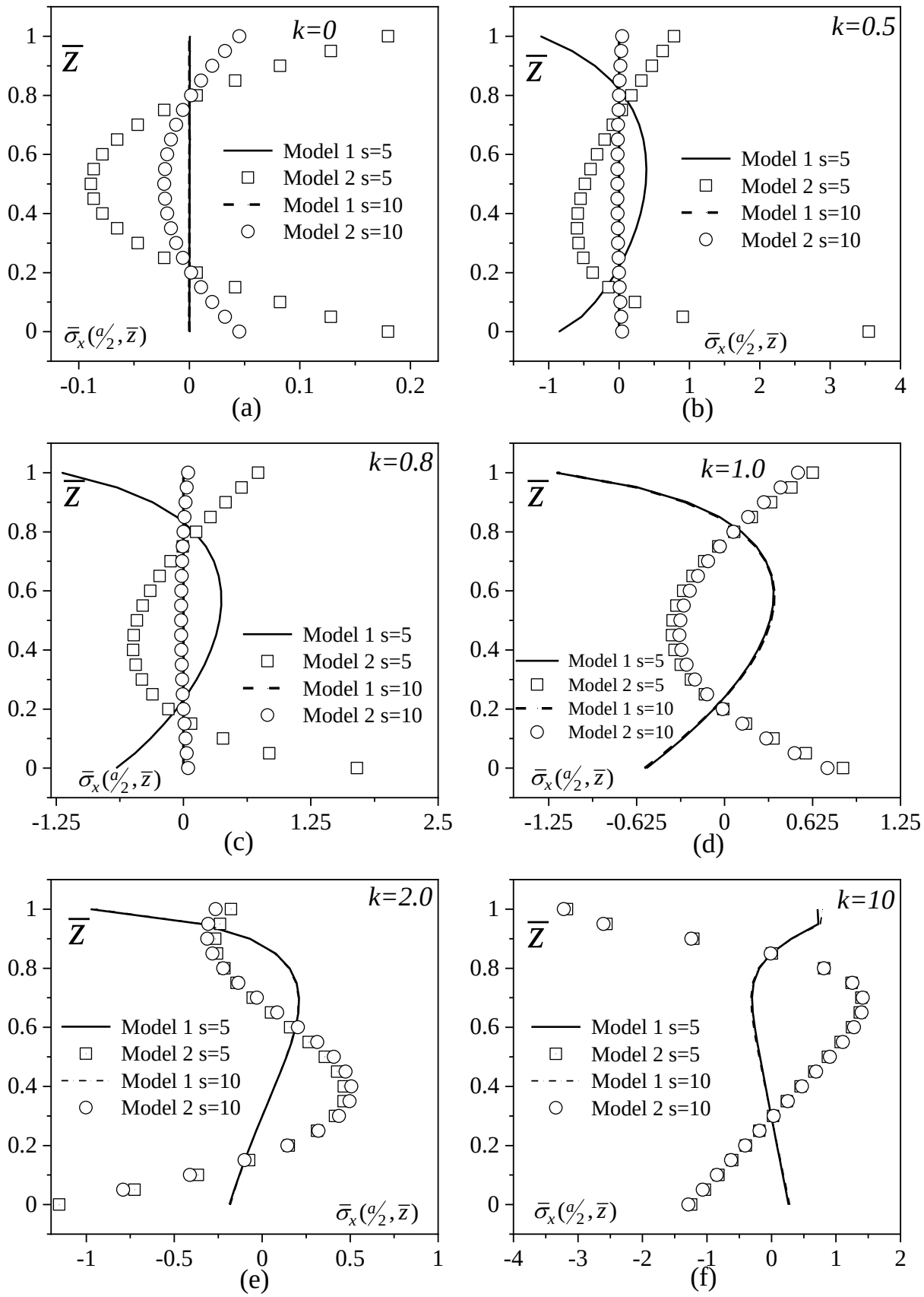

Fig. 7. Thickness variation of normalized in-plane stresses ($\bar{\sigma}_x$) for various graded FG laminate [Material set C].

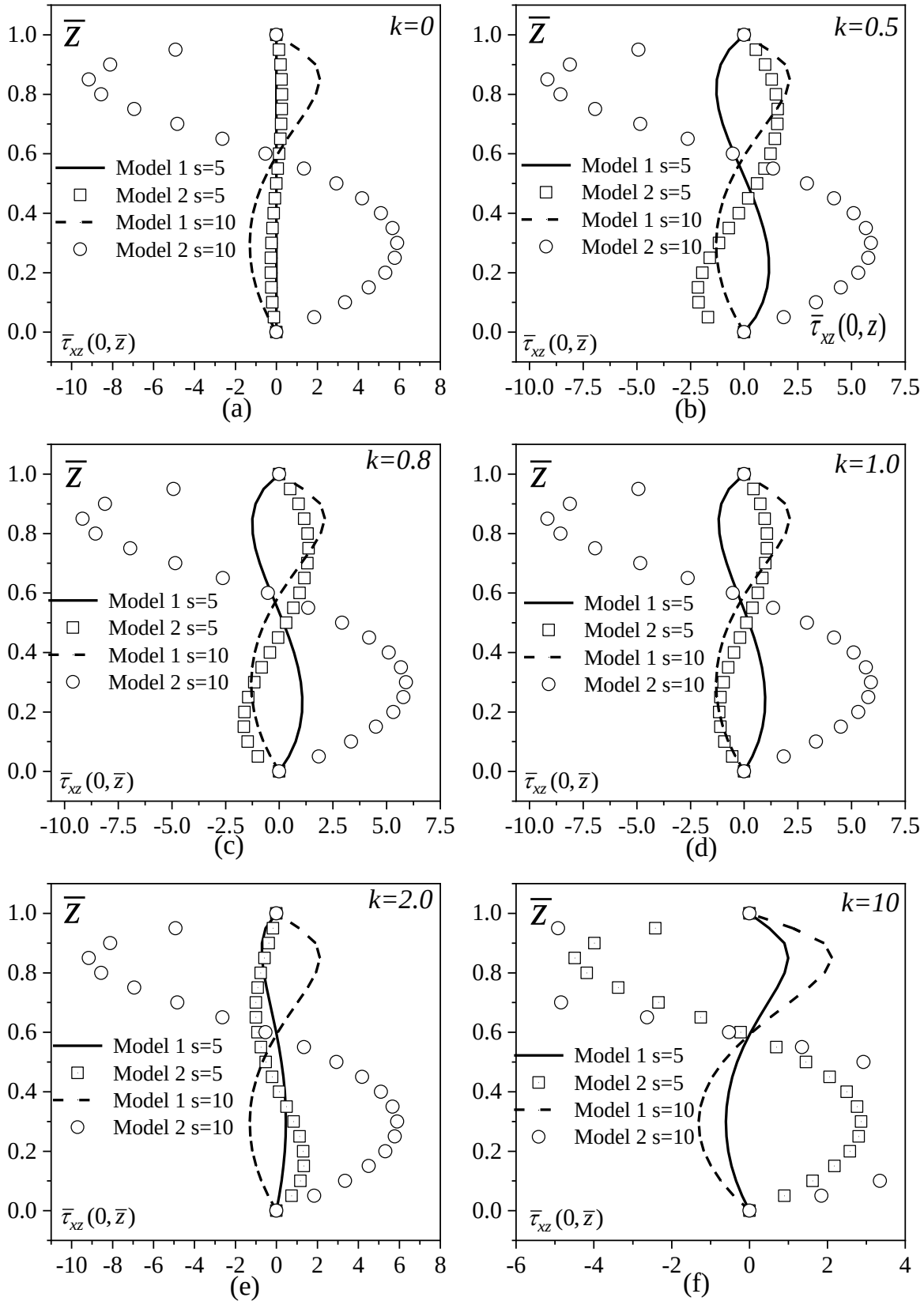

Fig. 8. Thickness variation of normalized transverse stresses ($\overline{\tau}_{xz}$) for various graded FG laminate [Material set C].

6. Concluding remarks

Semi-analytical formulations based on a two-point boundary value problem governed by a set of coupled first-order ordinary differential equations (ODEs) and free from simplified assumptions along the thickness of laminates for heat conduction equation and stress analysis have discussed in this paper. The present formulation involves using analytical and numerical approaches, which achieves both accuracy and simplicity. It also helps to reduce the dimension of the elasticity problem and helps to avoid a complex 3D stress analysis.

Comparison between power law varied temperature fields along the depth of a laminate and temperature field obtained through heat conduction solutions have documented for different material combinations as well for various aspect ratios. The existence of material sensitivity has been noticed for temperature profile and the thickness of a laminate, Whereas no observation noted the effect of aspect ratio. Further, stress analyses performed and document for both thermal and thermomechanical loading. Considerable differences have been seen during stress analysis for the thermal load on various parameters from displacement and stress groups. In contrast, no significant difference had recorded for stress analysis with thermomechanical loading.

References

[1] Chakraborty A, Gopalakrishnan S, Reddy JN. A new beam finite element for the analysis of functionally graded materials. Int J Mech Sci 2003;45:519–39. doi:10.1016/S0020-7403(03)00058-4.

[2] Benatta MA, Mechab I, Tounsi A, Adda Bedia EA. Static analysis of functionally graded short beams including warping and shear deformation effects. Comput Mater Sci 2008;44:765–73. doi:10.1016/j.commatsci.2008.05.020.

[3] Kadoli R, Akhtar K, Ganesan N. Static analysis of functionally graded beams using higher order shear deformation theory. Appl Math Model 2008;32:2509–25. doi:10.1016/j.apm.2007.09.015.

[4] Ben-Oumrane S, Abedlouahed T, Ismail M, Mohamed BB, Mustapha M, El Abbas AB. A theoretical analysis of flexional bending of Al/Al2O3 S-FGM thick beams. Comput Mater Sci 2009;44:1344–50. doi:10.1016/j.commatsci.2008.09.001.

[5] Mahi A, Adda Bedia EA, Tounsi A, Mechab I. An analytical method for temperature-dependent free vibration analysis of functionally graded beams with general boundary conditions. Compos Struct 2010;92:1877–87. doi:10.1016/j.compstruct.2010.01.010.

[6] Kiani Y, Eslami MR. Thermal buckling analysis of functionally graded material beams. Int J Mech Mater Des 2010;6:229–38. doi:10.1007/s10999-010-9132-4.

[7] Wattanasakulpong N, Gangadhara Prusty B, Kelly DW. Thermal buckling and elastic vibration of third-order shear deformable functionally graded beams. Int J Mech Sci 2011;53:734–43. doi:10.1016/j.ijmecsci.2011.06.005.

[8] Giunta G, Crisafulli D, Belouettar S, Carrera E. Hierarchical theories for the free vibration analysis of functionally graded beams. Compos Struct 2011;94:68–74. doi:10.1016/j.compstruct.2011.07.016.

[9] Ma LS, Lee DW. A further discussion of nonlinear mechanical behavior for FGM beams under in-plane thermal loading. Compos Struct 2011;93:831–42. doi:10.1016/j.compstruct.2010.07.011.

[10] Thai H-T, Vo TP. Bending and free vibration of functionally graded beams using various higher-order shear deformation beam theories. Int J Mech Sci 2012;62:57–66. doi:10.1016/j.ijmecsci.2012.05.014.

[11] Thai H-T, Vo TP. A nonlocal sinusoidal shear deformation beam theory with application to bending, buckling, and vibration of nanobeams. Int J Eng Sci 2012;54:58–66. doi:10.1016/j.ijengsci.2012.01.009.

[12] Ma LS, Lee DW. Exact solutions for nonlinear static responses of a shear deformable FGM beam under an in-plane thermal loading. Eur J Mech - A/Solids 2012;31:13–20. doi:10.1016/j.euromechsol.2011.06.016.

[13] Şimşek M, Reddy JN. Bending and vibration of functionally graded microbeams using a new higher order beam theory and the modified couple stress theory. Int J Eng Sci 2013;64:37–53. doi:10.1016/j.ijengsci.2012.12.002.

[14] Li S-R, Cao D-F, Wan Z-Q. Bending solutions of FGM Timoshenko beams from those of the homogenous Euler–Bernoulli beams. Appl Math Model 2013;37:7077–85. doi:10.1016/j.apm.2013.02.047.

[15] Lezgy-Nazargah M. Fully coupled thermo-mechanical analysis of bi-directional FGM beams using NURBS isogeometric finite element approach. Aerosp Sci Technol 2015;45:154–64. doi:10.1016/j.ast.2015.05.006.

[16] El-Ashmawy AM, Kamel MA, Elshafei MA. Thermo-mechanical analysis of axially and transversally Function Graded Beam. Compos Part B Eng 2016;102:134–49. doi:10.1016/j.compositesb.2016.07.015.

[17] Trinh LC, Vo TP, Thai H-T, Nguyen T-K. An analytical method for the vibration and buckling of functionally graded beams under mechanical and thermal loads. Compos Part B Eng 2016;100:152–63. doi:10.1016/j.compositesb.2016.06.067.

[18] De Pietro G, Hui Y, Giunta G, Belouettar S, Carrera E, Hu H. Hierarchical one-dimensional finite elements for the thermal stress analysis of three-dimensional functionally graded beams. Compos Struct 2016;153:514–28. doi:10.1016/j.compstruct.2016.06.012.

[19] Hui Y, Giunta G, Belouettar S, Huang Q, Hu H, Carrera E. A free vibration analysis of three-dimensional sandwich beams using hierarchical one-dimensional finite elements. Compos Part B Eng 2017;110:7–19. doi:10.1016/j.compositesb.2016.10.065.

[20] Rajasekaran S, Khaniki HB. Bi-directional functionally graded thin-walled non-prismatic Euler beams of generic open/closed cross section Part I: Theoretical formulations. Thin-Walled Struct 2019;141:627–45. doi:10.1016/j.tws.2019.02.006.

[21] Pendhari SS, Kant T, Desai YM, Venkata Subbaiah C. On deformation of functionally graded narrow beams under transverse loads. Int J Mech Mater Des 2010;6:269–82. doi:10.1007/s10999-010-9136-0.

[22] Kantrovich LV, Krylov VI. Approximate Methods of Higher Analysis, 3rd Edition, Noordhoff, Groningen,. 1958.